



Improving the catalytic activity of formate dehydrogenase from *Candida boidinii* by using magnetic nanoparticles

Caterina G.C.M. Netto^a, Marcelo Nakamura^a, Leandro H. Andrade^b, Henrique E. Toma^{a,*}

^a Supramolecular NanotechLab, Institute of Chemistry, University of São Paulo, São Paulo, SP, Brazil

^b Laboratory of Fine Chemistry and Biocatalysis, Institute of Chemistry, University of São Paulo, São Paulo, SP, Brazil

ARTICLE INFO

Article history:

Available online 6 April 2012

Keywords:

Formate dehydrogenase

Immobilization

Magnetic nanoparticles

ABSTRACT

Formate dehydrogenase from *Candida boidinii* (FDH) was immobilized on three different magnetic supports: one composed by magnetite nanoparticles directly silanized with APTS (aminopropyltriethoxysilane), i.e. MagNP-APTS; the second one containing a silica gel coated magnetite core which was further silanized with APTS (MagNP@SiO₂-APTS), and the third one consisting of magnetite-APTS coated with Glyoxyl-agarose (MagNP-Glyoxyl-agarose). The catalytic activity of the three FDH systems was investigated as a function of pH and temperature. The silica gel coated nanoparticles provided the highest conversion rates; however, in terms of recycling, magnetite without the silica shell led to the most stable system. By using the enzyme tryptophan residues as internal fluorescence probes, the structure-activity behavior was investigated in the presence of the formate and NAD⁺ substrates, revealing a rather contrasting behavior in the three cases. Because of its peculiar behavior, a direct interaction of the magnetic nanoparticles with the catalytic sites seems to be implicated in the case of MagNP-APTS.

© 2012 Elsevier B.V. All rights reserved.

1. Introduction

Immobilization has effectively been used as a method for increasing the stability of enzymes and many reports have also suggested the possibility of improving the enzyme activity and selectivity [1,2]. Several material supports and methods have already been studied, but in particular magnetic nano (or micro) particles seem especially attracting since they can be easily recovered by the use of an external magnet. In addition, the use of an immobilized enzyme [3–5] introduces a great simplification on the reactor design and control of the reactions, since the simple removal of the enzyme effectively allows to stop the process. This advantage is stimulating the use of magnetic nanoparticles in biocatalysis.

The conversion of CO₂ to formate in biological systems is typically performed by a NADH dependent enzyme called formate dehydrogenase (FDH), which is also used for catalytical studies involving hydride transfer, due to the substrate simplicity. A typical biotechnological use of FDH is in the determination of formic and oxalic acid in solution, but it can also be used as a NAD⁺ regeneration system [6–8], especially after immobilization, e.g. on silica matrixes [9], agaroses [1,10], membranes [11] and magnetic nanoparticles [12]. The best recyclability performance has been obtained using alginate gels as supports [13]. Another important feature of this

enzyme is its role as one of the catalysts in the enzymatic conversion of CO₂ to methanol [14–16], which is important for the development of new routes to fabrication of fuels and chemicals.

In spite of the previous studies on FDH immobilization in the literature [17], a systematic study focusing on the improvement of the enzyme activity and stability in immobilized systems is yet missing.

Hence, we performed the immobilization of FDH from *Candida boidinii* on three types of functionalized magnetite nanoparticles: MagNP-APTS, MagNP@SiO₂-APTS and MagNP-Glyoxyl-agarose, pursuing the understanding of the relevant parameters for improving the performance and recycling the FDH enzyme.

2. Experimental

All reagents were purchased from Sigma–Aldrich and used without previous purification.

Formate dehydrogenase from *C. boidinii* exhibited 5–15 units/mg of protein. One unit expresses the oxidation of 1 μmol of formate to CO₂ in the presence of NAD⁺ at pH 7.6 and 37 °C.

2.1. Synthesis of MagNP, MagNP@SiO₂ and silanized MagNPs

The magnetic nanoparticles were prepared by the co-precipitation method, and their silanization was described elsewhere [18].

* Corresponding author.

E-mail address: henetoma@iq.usp.br (H.E. Toma).

2.2. Glyoxyl-agarose synthesis

The synthesis of glyoxyl-agarose was performed as described by Manrich et al. [19].

2.3. General procedure of FDH immobilization on MagNP-APTS

The enzyme stock solution consisted of 3.13 mg/mL FDH in Tris–HCl 0.1 M (pH 7.5) buffer. For the immobilization step, 300 μ L of this solution (0.94 mg, 5 U) was mixed with 500 μ L of Tris–HCl 0.1 M buffer containing MagNP-APTS (1, 2, 4, 8 and 16 mg). Then, glutaraldehyde (1.2 μ mol, 2.4 μ mol, 4.8 μ mol, 9.6 μ mol or 19.2 μ mol) was added and allowed to react at 0 °C for a determined period of time (0, 2, 5, 10, 15, 20 and 60 min). The immobilized enzymes were confined by using an external miniature Nd₂Fe₁₄B magnet (1 cm³, 11 kOe from MagTek), and washed 3 times with 0.5 mL of Tris–HCl 0.1 M buffer solution. The best conditions were obtained by using 16 mg of MagNP-APTS, 1.2 μ mol of glutaraldehyde and 1 h of immobilization.

2.4. General procedure of FDH immobilization on MagNP@SiO₂-APTS

As in the preceding case, MagNP@SiO₂-APTS (1, 2, 4, 8, 13, 16 and 18 mg) was suspended into 0.5 mL of Tris–HCl 0.1 M buffer, and 300 μ L of the FDH stock solution (0.94 mg, 5 U) was added, followed by 1.2% glutaraldehyde aqueous solution (0, 0.6 μ mol, 1.2 μ mol, 2.4 μ mol, 4.8 μ mol, 9.6 μ mol or 19.2 μ mol). The mixture was allowed to react at 0 °C during 0, 2, 5, 10, 15 or 20 min. After confining the immobilized enzymes by using an external miniature magnet, the particles were washed 3 times with 0.5 mL Tris–HCl 0.1 M of buffer solution. The best conditions were obtained with 13 mg of MagNP@SiO₂-APTS, 0.6 μ mol of glutaraldehyde and 10 min of immobilization.

2.5. General procedure of FDH immobilization on MagNP-APTS/Glyoxyl-Agarose

In this case, 8 mg of MagNP-APTS and 300 μ L of the FDH stock solution (0.94 mg, 5 U) were mixed with 700 μ L of Tris–HCl buffer solution (0.1 M) and 300 μ L of glyoxyl-agarose (100 mg/mL) was added. The immobilization was allowed to proceed for 10 min at 0 °C. Then, by using an external miniature magnet, the particles were washed 3 times with 0.5 mL of buffer and finally dispersed into 0.6 mL of the buffer solution.

2.6. Formate conversion to CO₂

The magnetic-FDH was transferred into a cuvette containing 1 mL of Tris–HCl buffer solution (0.1 M). Then 10 μ L of 0.4 M sodium formate and 5 μ L of NAD⁺ (0.9 mM) were added. The kinetics of formation of NADH was monitored at 340 nm.

2.6.1. Temperature and pH dependence studies

pH dependence studies were performed at 37 °C. For the temperature studies, the pH was kept at 7.5.

2.6.2. Recycling studies

For the recycling studies, MagNP-APTS/FDH were used at pH 7.5 and 22 °C, MagNP@SiO₂-APTS/FDH and MagNP-APTS/Glyoxyl-Agarose/FDH were used at pH 7.5 and 27 °C, corresponding to their best performance conditions.

2.6.3. Thermodynamic studies

K_M measurements were performed in 0.1 M Tris–HCl buffer, pH 7.5, employing 50 μ L of NAD⁺ (0.9 mM) and 40 mM of formate, at

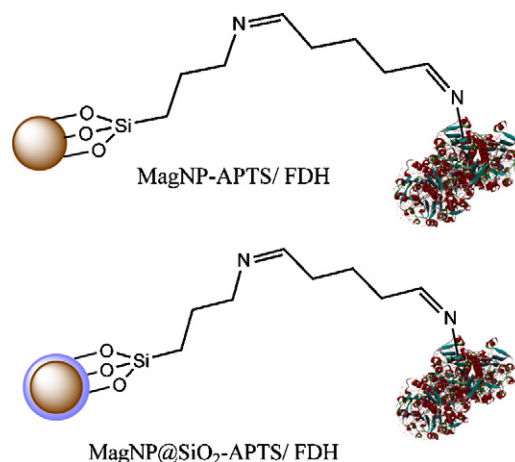


Fig. 1. Covalent binding of the enzyme (FDH) to magnetic particles via glutaraldehyde (structures not in scale).

20 °C. ΔH^\ddagger and ΔS^\ddagger measurements were performed at 20, 21, 22, 23 and 25 °C and pH 7.5.

2.7. Physical measurements

UV–VIS spectrophotometry measurements were carried out on a Hewlett Packard 8453-A diode-array spectrophotometer.

For atomic force microscopy (AFM) measurements 5 μ L of nanoparticle solution were deposited over mica (Ted Pella Inc.), and allowed to dry in a clean laminar flow chamber. The AFM images were obtained using a PicoSPM I microscope (Molecular Imaging, MI) with PicoScan 2100 (MI) controller coupled with MACMode (MI) unit for intermittent contact AFM and MAC Mode SFM. Data acquisition were obtained using a PicoScan (M.I) device with the scan rate between 0.5 and 1.0 Hz operating from 256 to 512 points per line. For the AFM and MACMode SFM measurements, silicon tips with high aspect ratio from Nanosensors and Agilent (Type II MACLevers, $k \sim 2.8$ N/m; $f \sim 60$ kHz) were employed.

Fluorescence measurements were recorded on a Photon Technology International Inc. model LS-100 spectrofluorometer.

3. Results and discussion

Magnetic nanoparticles obtained by the co-precipitation method were silanized with aminopropyltriethoxysilane and reacted with glutaraldehyde in order to form imino bounds between the enzyme and nanoparticle. Both particles, MagNP-APTS and MagNP@SiO₂-APTS were submitted to similar immobilization methodologies, differing only in the inner shell composition and particle size, while the method using glyoxyl-agarose as a “substitute” for glutaraldehyde, involved a multi-point covalent immobilization.

3.1. Optimization of the immobilization methodology

The best FDH-magnetic particle system was achieved after several immobilization optimizations, which resulted in a different protocol for each support.

3.1.1. Immobilization by glutaraldehyde

The immobilization of formate dehydrogenase on magnetic nanoparticles by the glutaraldehyde method results in systems similar to those shown in Fig. 1.

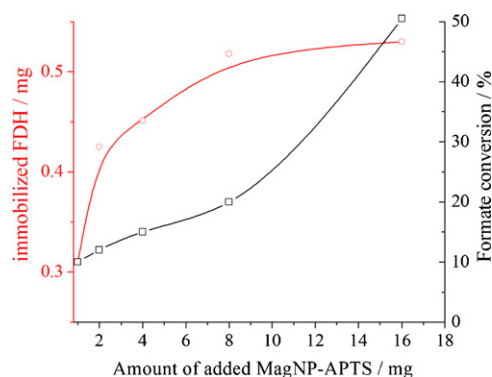


Fig. 2. Relation between the amount of immobilized FDH (red line) and formate conversion (black line) to the amount of MagNP-APTS in the immobilization process. (For interpretation of the references to color in this figure legend, the reader is referred to the web version of the article.)

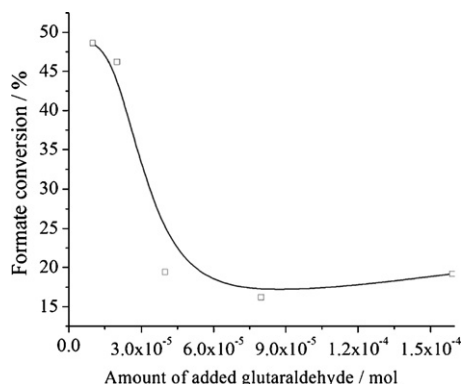


Fig. 3. Effect of the amount of glutaraldehyde on the formate conversion.

The first variable to be analyzed was the amount of added MagNP-APTS. Keeping the concentration of 0.2 M of glutaraldehyde and 5 min of immobilization time, we observed that 0.5 mg of FDH was immobilized on 8 mg and 16 mg of particles; however, the formate conversion increased by a factor of two when 16 mg of MagNP-APTS were used (Fig. 2).

By increasing the amount of glutaraldehyde in the immobilization process, the immobilized enzyme exhibited a decreased activity, as shown in Fig. 3. Accordingly, we have chosen 1.5×10^{-5} mol of glutaraldehyde as the best value.

The increase in the immobilization time improved the yields of formate conversion, reaching a maximum rate at 1 h (80% formate conversion) as shown in Fig. 4. After this time, the enzyme activity decreased drastically.

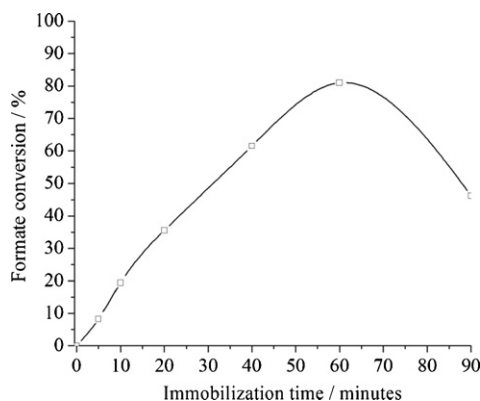


Fig. 4. Relation between the immobilization time and formate conversion.

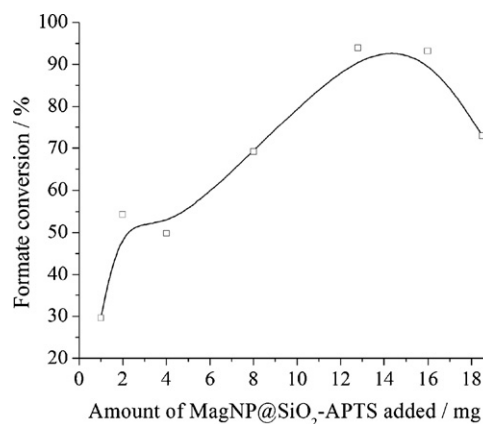


Fig. 5. Relation between the amount of MagNP@SiO₂-APTS added to the immobilization process and the formate conversion.

For the MagNP@SiO₂-APTS particles, by increasing their amount in the immobilization process, keeping the same amount of FDH (0.94 mg, 5 U), a gradual increase of conversion was observed up to 13 mg of nanoparticles. After this point, the formate conversion decreased, as shown in Fig. 5.

We observed two maximum peaks in relation to the immobilization time, one at 2 min and the other at 10 (Fig. 6). For this reason, the influence of the amount of glutaraldehyde was investigated for the two periods of time. For the two minutes peak, the addition of glutaraldehyde decreased the formate conversion, corresponding to a possible adsorption of FDH on the particles surface, while for 10 min of immobilization, 5 μ mol of glutaraldehyde gives the best conversion performance and suggests also the formation of covalent bounds between enzyme and support (Fig. 7).

3.1.2. Immobilization by glyoxyl-agarose

The enzyme (FDH) was covalently attached to glyoxyl-agarose and MagNP-APTS resulting in MagNP-APTS/Glyoxyl-Agarose/FDH, as illustrated in Fig. 8.

Formate dehydrogenase immobilized on magnetic glyoxyl-agarose support suffered a decrease in formate conversion with the increase in immobilization time (Fig. 9). For this reason, the best adopted protocol was the rapid mixture of the two components. This short period of time was apparently enough for binding the support and enzyme, producing no negative effect on the FDH conformation.

From the suspension obtained after the immobilization protocol, accurate volumes were employed for the reaction. It was observed that the increase in concentration of MagNP-Glyoxyl-Agarose/FDH in the reaction mixture leads to an increase

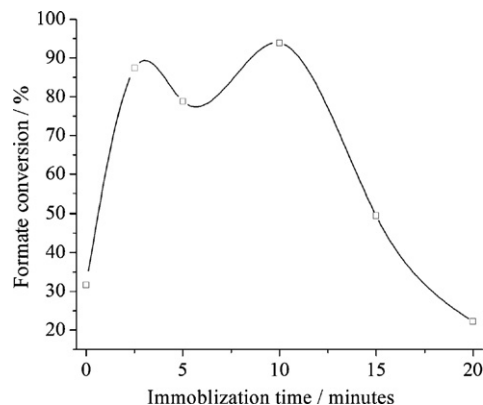


Fig. 6. Immobilization time influence on the formate conversion.

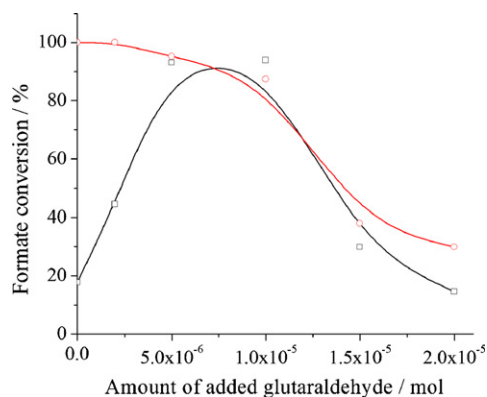


Fig. 7. Effect of the amount of glutaraldehyde on the formate conversion for 2 min (red line) and 10 min of immobilization (black line). (For interpretation of the references to color in this figure legend, the reader is referred to the web version of the article.)

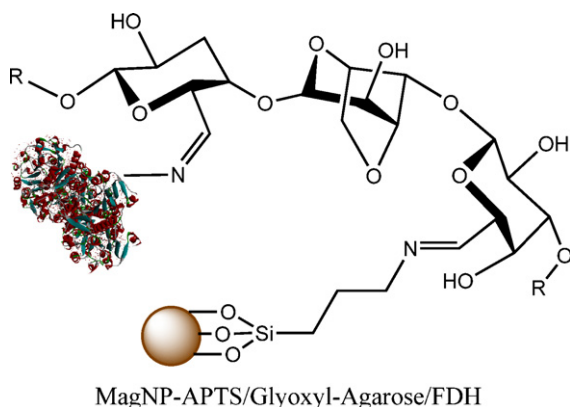


Fig. 8. Covalent binding of the enzyme (FDH) to magnetic particles using glyoxyl-agarose.

in conversion, reaching 94% for 200 μ L of MagNP-Glyoxyl-Agarose/FDH (Fig. 10).

3.2. Morphology

The morphology of the films was analyzed by atomic force microscopy in order to verify the homogeneity and size. After drying over mica the AFM phase contrast image (Fig. 11B) of MagNP-APTS/FDH revealed agglomerates of about 0.5–2 μ m comprising small inorganic clusters anchored on the enzyme

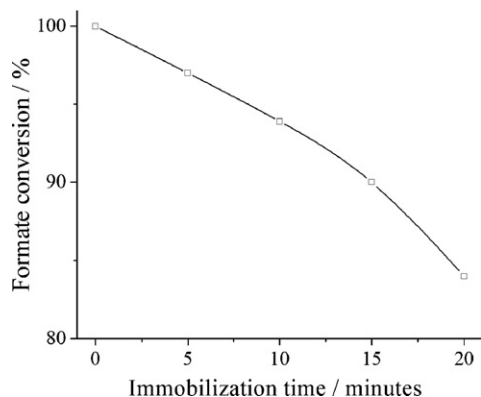


Fig. 9. MagNP-Glyoxyl-Agarose/FDH system: relation of immobilization time with the formate conversion.

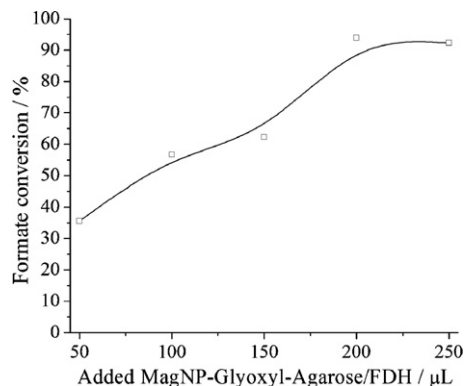


Fig. 10. MagNP-Glyoxyl-Agarose/FDH system: relation of enzymatic system amount with formate conversion.

conglomerate. In contrast, for the MagNP@SiO₂-APTS/FDH system (Fig. 12) the observed poor phase contrast indicated that the magnetic nanoparticles are surrounded by the enzyme. In the case of MagNP-APTS/Glyoxyl-Agarose/FDH, although the phase contrast image shows some magnetic nanoparticles exposed at the surface (Fig. 13B), presumably most of them should be covered by the agarose and enzyme coating.

3.3. Temperature and pH dependence studies

These FDH-magnetic particles were used in catalytic studies at different pH and temperatures. Free FDH seems to have a nearly constant activity for formate conversion, around 40%, in the range of pH from 5.8 to 8.8. In the case of MagNP@SiO₂-APTS/FDH an optimum pH around 7.5 is clearly defined, increasing the conversions up to 90%. In contrast, for MagNP-APTS/Glyoxyl-Agarose/FDH the conversion remains practically constant, around 20%, between pH 5.8 and 8.8. On the other hand, MagNP-APTS/FDH exhibits a contrasting catalytic profile, starting with negligible conversion rates at low pHs, but increasing rapidly above pH 7.5 and reaching 90% conversion at pH 9.8 (Fig. 14).

In the temperature dependence studies, although the best performance for free FDH was 37 $^{\circ}$ C, corresponding to 35% of formate conversion, this enzyme seemed quite robust to temperature variation (Fig. 15) since it didn't loose much activity upon heating up to 47 $^{\circ}$ C (32% of formate conversion). When immobilized on MagNP-APTS and MagNP@SiO₂-APTS, formate dehydrogenase gave higher conversions, but became more sensitive to temperature changes. MagNP-APTS/FDH was more active at temperatures higher than 37 $^{\circ}$ C with an optimum temperature at 42 $^{\circ}$ C, while MagNP@SiO₂-APTS/FDH exhibited higher conversions in the 23–37 $^{\circ}$ C interval. The immobilization through glyoxyl-agarose rendered FDH very sensitive to the temperature, shifting the maximum conversion temperature to 27 $^{\circ}$ C.

3.4. Recycle

When submitted to recycle, all the three systems exhibited about 30% decay from the original activity after the first cycle, keeping afterwards a constant activity, at least for the next five cycles. The relative activity of MagNP@SiO₂/FDH (green bars, Fig. 16) was always significantly higher during the five initial cycles, while MagNP-APTS/Glyoxyl-Agarose/FDH (red bars, Fig. 16) exhibited the smallest activity. In both cases, a sharp decrease was observed for the activity after the 6th cycle (Fig. 16). The MagNP-APTS/FDH system (blue bars, Fig. 16) exhibited a more stable behavior, maintaining its activity around 40% up to 10 successive cycles.

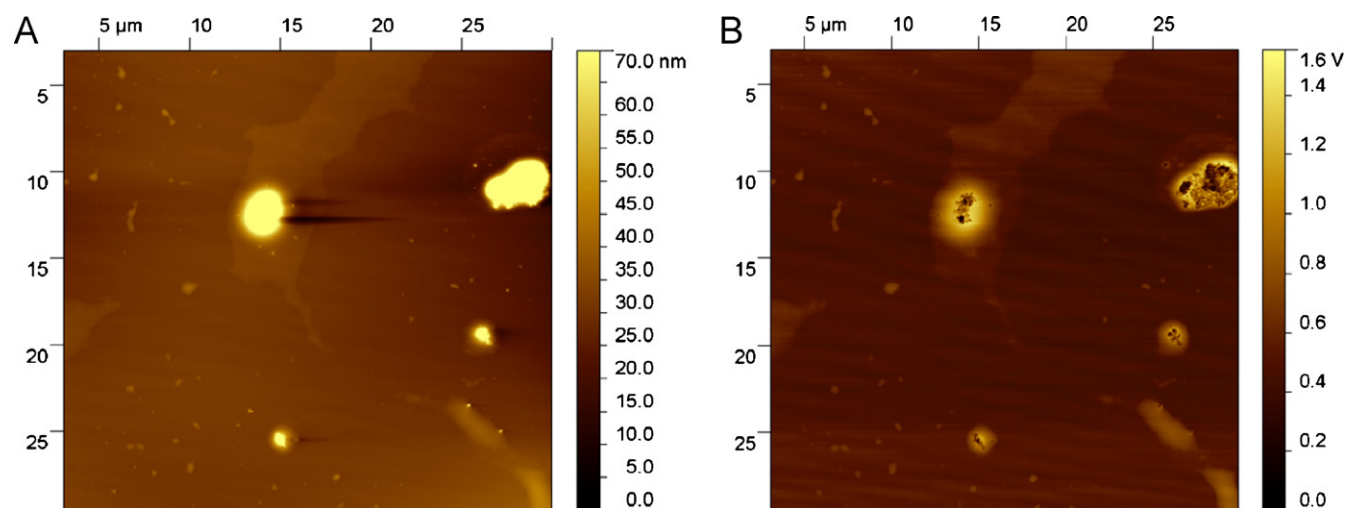


Fig. 11. Atomic force microscopy images of MagNP-APTS/FDH (A) topography and (B) phase contrast.

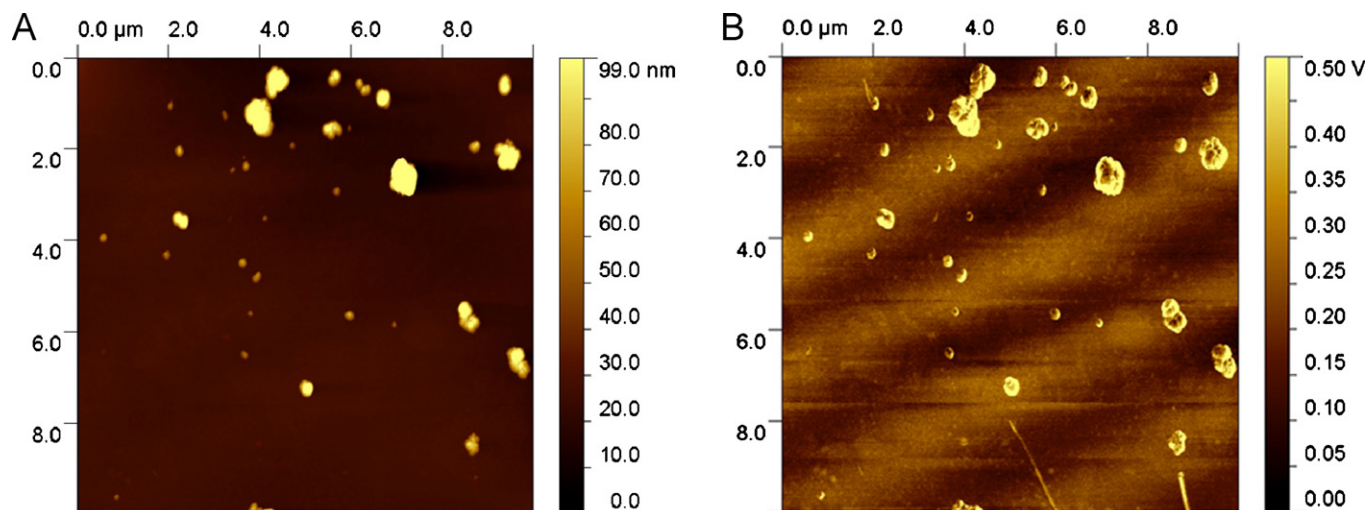


Fig. 12. Atomic force microscopy images of MagNP@SiO₂-APTS/FDH (A) topography and (B) phase contrast.

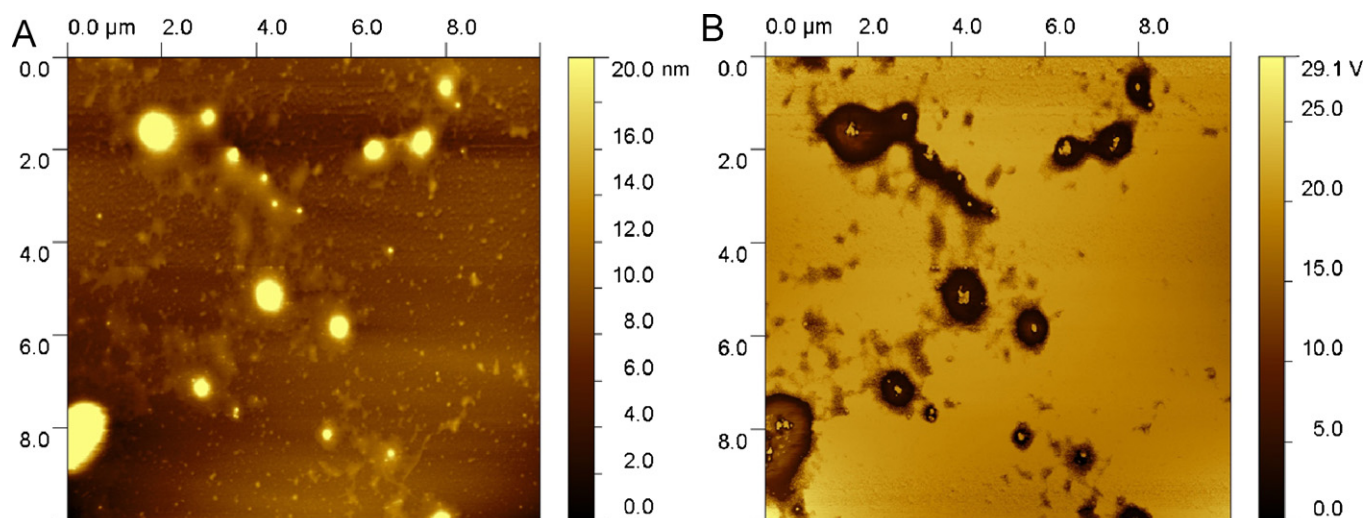


Fig. 13. Atomic force microscopy images of MagNP-APTS/Glyoxyl-Agarose/FDH (A) topography and (B) phase contrast.

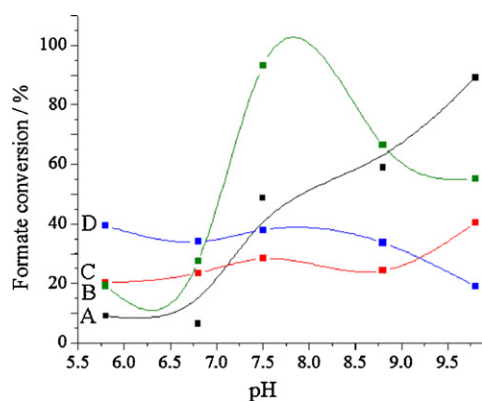


Fig. 14. Enzyme activity in relation to pH for free FDH (line D), MagNP-Glyoxyl-Agarose/FDH (line C), MagNP-APTS/FDH (line A) and MagNP@SiO₂-APTS/FDH (B).

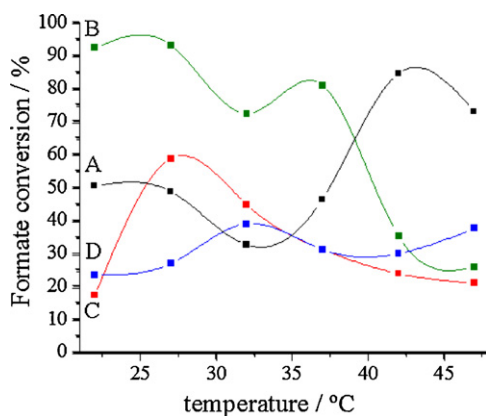


Fig. 15. Enzyme activity in relation to temperature for free FDH (blue line, D), MagNP-Glyoxyl-Agarose/FDH (red line, C), MagNP-APTS/FDH (black line, A) and MagNP@SiO₂-APTS/FDH (green line, B). (For interpretation of the references to color in this figure legend, the reader is referred to the web version of the article.)

3.5. Thermodynamic properties

Activation energy and entropy were obtained for the nanoparticles/enzyme and free enzyme pursuing additional clues on how the immobilization can influence the enzyme activity. As shown in Table 1, the higher activity observed for MagNP-APTS/FDH is accompanied by the decrease of the Michaelis–Menten constant, K_M by a factor of two. The observed decrease in the activation energy would reflect a favorable influence of the catalytic site, however this is more than compensated by the decrease of activation entropy, implying in a more organized structure. The best compromise between the activation energy and entropy was observed for MagNP-APTS/FDH system. For the MagNP@SiO₂-APTS/FDH system,

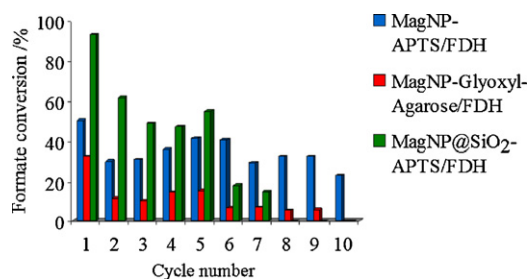


Fig. 16. Recycling, in sequence presentation, of MagNP-APTS/FDH (blue line), MagNP-Glyoxyl-Agarose/FDH (red line) and MagNP@SiO₂-APTS/FDH (green line), respectively. (For interpretation of the references to color in this figure legend, the reader is referred to the web version of the article.)

Table 1

Difference of K_M , ΔH^\ddagger and ΔS^\ddagger for free and immobilized FDH.

	Activity (U) ^a	K_M (mM) ^b	ΔH^\ddagger ^c	ΔS^\ddagger ^d
Free FDH	5	6	13	−78
MagNP-APTS/FDH	4	3	8.6	−104
MagNP@SiO ₂ -APTS/FDH	12	20	5.9	−115
MagNP-APTS/Glyoxyl agarose/FDH	6	9	21	−120

^a 27 °C, pH 7.5.

^b 20 °C, Tris–HCl buffer (0.1 M pH 7.5), 5 μ L of NAD⁺ (0.9 mM) and 40 mM of formate.

^c kJ mol^{−1}.

^d J mol^{−1} K^{−1}.

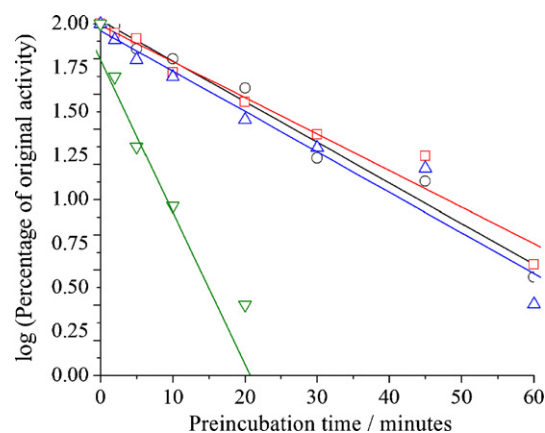


Fig. 17. Enzyme inactivation at 60 °C and pH 7.5. Free FDH (○), MagNP-APTS/FDH (□), MagNP@SiO₂-APTS/FDH (Δ) and MagNP-APTS/Glyoxyl-Agarose/FDH (▽).

the smaller activation enthalpy was compensated by the increase of K_M , while in the case of MagNP-APTS/Glyoxyl-Agarose/FDH all the factors involved are less favorable in relation to the free enzyme.

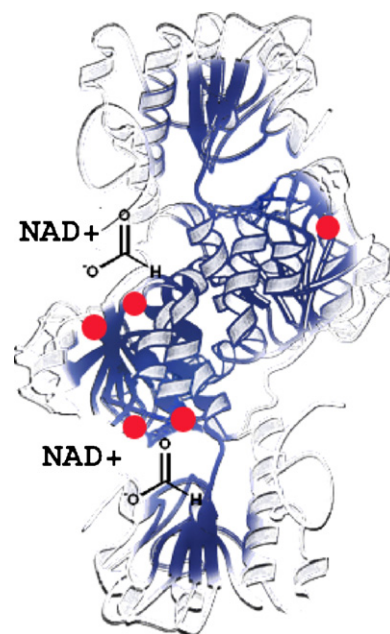


Fig. 18. Scheme of FDH from *Candida boidinii* showing the tryptophans sites (red circles). (For interpretation of the references to color in this figure legend, the reader is referred to the web version of the article.)

Adapted from [22].

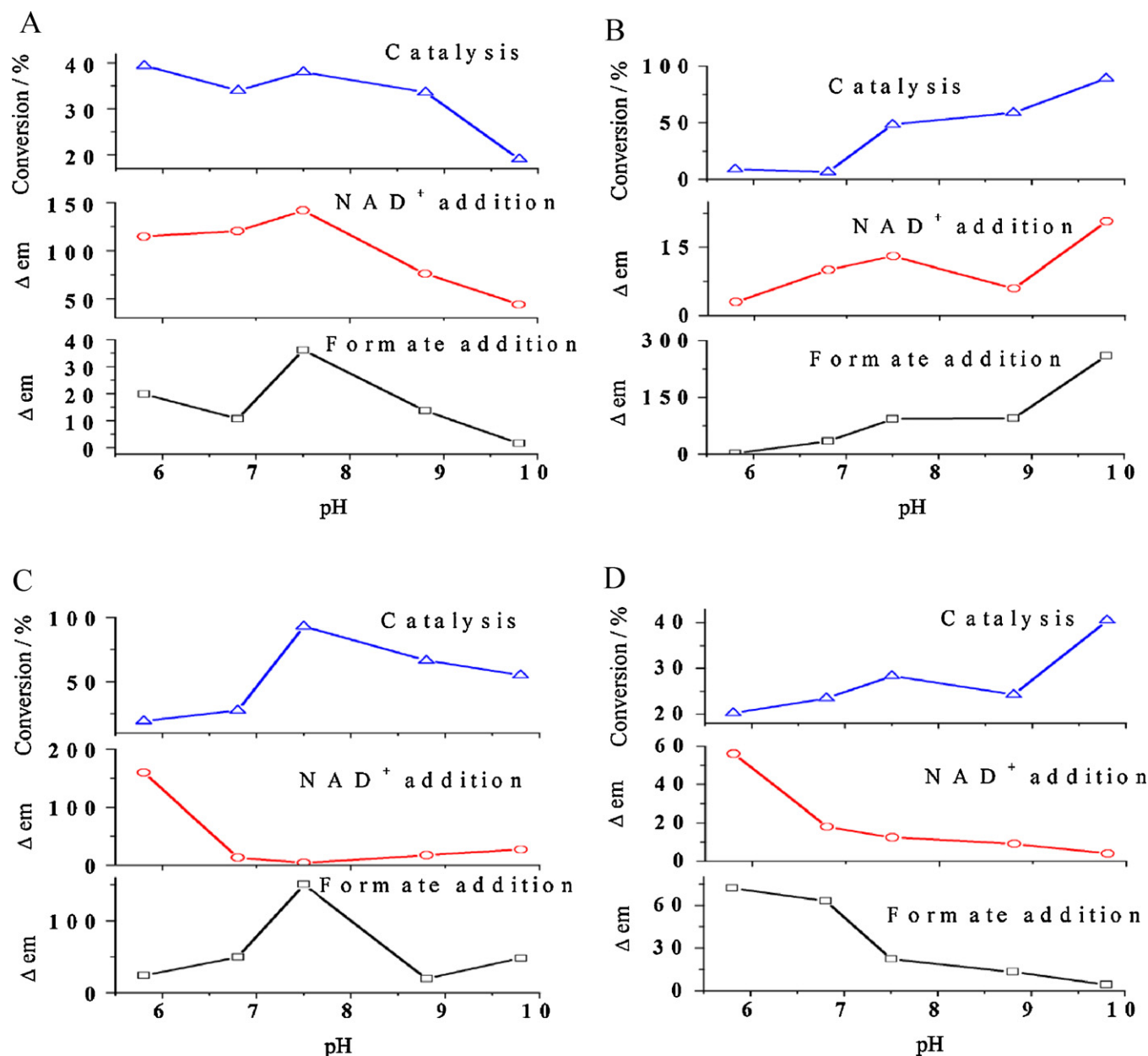


Fig. 19. Relation between the catalysis at different pH (blue line, Δ) and the magnitude of quenching from original tryptophan emission before and after addition of formate (black line, \square) and NAD⁺ (red line, \circ) for (A) free FDH, (B) MagNP-APTS/FDH, (C) MagNP@SiO₂-APTS/FDH and (D) MagNP-APTS/Glyoxyl-Agarose/FDH. (For interpretation of the references to color in this figure legend, the reader is referred to the web version of the article.)

3.6. Enzyme stability

In order to check for the enzyme stability, they were pre-incubated for a period of time up to 1 h, at 60 °C and pH 7.5, and their activity evaluated. The slope values for free FDH and MagNP@SiO₂-APTS were rather similar (-0.023 min^{-1}), while MagNP-APTS/FDH exhibited a smaller slope value (-0.020 min^{-1}) indicating an increase in FDH stability. MagNP-APTS/Glyoxyl-Agarose/FDH presented a slope value of -0.086 min^{-1} , being completely inactive after 20 min of incubation (Fig. 17).

3.7. Structure–activity dependence

Tryptophan exhibits a characteristic fluorescence in the visible (from 300 to 350 nm) upon excitation at 280 nm. The emission is particularly sensitive to local electric fields and has been used

to probe the substrate binding, undergoing quenching and shifts [20–23]. The difference in the emission intensity can be used for comparing the enzyme catalysis at different pHs, before and after the substrate and coenzyme addition.

Considering the FDH structure (PDB code, 2JCI), visualized with the Discovery Studio 2.5 program (Accelrys, San Diego, CA), the binding site possesses histidine, arginine and asparagine residues capable of forming H-bond with the oxygen atoms from formate. Histidine has already been proposed as a key residue directly involved in formate binding [24]. In the case of NAD⁺ binding, while isoleucine and valine provide a favorable hydrophobic environment, the adenine group can be sandwiched between an arginine and a cysteine, which are considered essential residues for coenzyme binding [23]. Actually, these residues can also determine how the catalysis will proceed at different pHs. In this sense, Blanchard and Cleland [25] reported that the binding of NAD⁺ is prevented by

the protonation of a group with $pK=6.4$ and by deprotonation of a group with $pK=8.4$. Such groups might be related with histidine and cysteine, respectively.

Another important point, as shown in Fig. 18, is that formate dehydrogenase from *C. boidinii* possesses 5 different tryptophans, four of them quite near the binding sites for NAD^+ and formate, while the other one is located far away from the binding sites. These tryptophans residues are indicated by red circles in Fig. 18.

As one can see in Fig. 19A, there is a good correlation between the changes in the tryptophan emission and the free enzyme activity after adding formate and NAD^+ , as a function of pH. The maximum activity is observed at pH 7.5 suggesting the participation of non-protonated histidine at this pH, in agreement with the hypothesis of Blanchard and Cleland [25]. The observed correlation means that the fluorescence changes from the tryptophan residues can effectively be used to probe the formate and NAD^+ binding sites in free FDH.

In the case of the enzyme immobilized on MagNP-APTS (Fig. 19B), the observed profiles are quite different from those of the free enzyme (Fig. 19A). The catalytic conversion increases with the pH (blue line, Fig. 19B), nearly paralleling the decay of the tryptophan emission in the presence of formate (black line, Fig. 19B) and NAD^+ , showing a negative fluctuation in this case, around pH 8.8, probably due to the deprotonation of the cysteine residue, as observed by Blanchard and Cleland [25]. MagNP-APTS/FDH- NAD^+ binary complex should have suffered an increase in its pK_a (originally 8.3–8.5) [25] since it must be protonated for the formate binding and the interaction of formate increases with increasing pH in this immobilized form of formate dehydrogenase. The observed tendency of increase with the pH (above pH 9) may reflect the involvement of additional sites, such as the residual amine groups from MagNP-APTS, since this effect is not observed for the free enzyme.

As shown in Fig. 19C, the catalytic profile of MagNP@SiO₂-APTS/FDH versus pH exhibits a maximum at pH 7.5, nearly coinciding with the fluorescence profile associated with the formate binding, as observed for the free enzyme (Fig. 19). In this case, NAD^+ binding seems to decrease accompanying the increase in pH (red line, Fig. 19C), but it is possible that the tryptophans are closer to the formate binding site and farther from NAD^+ site, hence, providing a less effective probe in this case.

In the third immobilization procedure (Fig. 19D), the pH activity profile of MagNP-APTS/Glyoxyl-Agarose/FDH system shows an increasing activity at increasing pHs, similar to that observed for MagNP-APTS (Fig. 19B). However, in this case, no coherent behavior was observed with respect to the fluorescence profiles in the presence of formate and NAD^+ . Agarose seems to mask the influence of the magnetic nanoparticles, and tryptophan is no longer a reliable probe for monitoring the active sites.

4. Conclusion

Immobilization of formate dehydrogenase from *C. boidinii* (FDH), on three different magnetic supports, represented

by MagNP-APTS, MagNP@SiO₂-APTS and MagNP-APTS/Glyoxyl-Agarose, resulted in a gain of enzymatic performance and stability. The silica gel coated nanoparticles (MagNP@SiO₂-APTS) provided the highest conversion rates (90% of formate conversion); however, in terms of recycling, magnetite without the silica shell (MagNP-APTS) led to the most stable system, with formate conversions around 40% for 10 successive cycles. MagNP-APTS/Glyoxyl-Agarose was consistently less active than the other two systems, exhibiting conversions of 30% and low temperature stability. By using the enzyme tryptophan residues as internal fluorescence probes, the structural–activity behavior was investigated in the presence of the formate and NAD^+ substrates, revealing a rather contrasting behavior in the three cases. A close interaction of the magnetic nanoparticles with the catalytic sites seems to be implicated in the case of MagNP-APTS. In the case of the agarose modified nanoparticle, the enzyme tryptophan residues seem to undergo non-specific quenching, precluding any reliable correlation with the catalytic sites.

Acknowledgements

The financial support from FAPESP and CNPq agencies is gratefully acknowledged.

References

- [1] J.M. Bolivar, L. Wilson, S.A. Ferrarotti, R. Fernandez-Lafuente, J.M. Guisan, C. Mateo, *Enzyme Microb. Technol.* 40 (2007) 540–546.
- [2] J.M. Guisan, *Immobilization of Enzymes and Cells*, 2nd ed., Humana Press Inc., New Jersey, 2006.
- [3] C. Mateo, J.M. Palomo, G. Fernandez-Lorente, J.M. Guisan, R. Fernandez-Lafuente, *Enzyme Microb. Technol.* 40 (2007) 1451–1463.
- [4] N.A. Kalkan, S. Akosoy, E.A. Akosoy, N. Hasirci, *J. Appl. Polym. Sci.* 123 (2012) 707–716.
- [5] T. Schmidt, C. Michalik, M. Zavrel, A. Spieß, W. Marquardt, M.B. Ansorge-Schumacher, *Biotechnol. Prog.* 26 (2010) 73–78.
- [6] M. Yoshimoto, R. Yamasaki, M. Nakao, T. Yamashita, *Enzyme Microb. Technol.* 46 (2010) 588–593.
- [7] Z.E. Shaked, G.M. Whitesides, *J. Am. Chem. Soc.* 102 (1980) 7105–7107.
- [8] H. Wu, Z.-Y. Jiang, S.-W. Xu, *Prepr. Pap.-Am. Chem. Soc., Div. Fuel Chem.* 48 (2003) 630.
- [9] J.M. Bolivar, L. Wilson, S.A. Ferrarotti, R. Fernandez-Lafuente, J.M. Guisan, C. Mateo, *Biomacromolecules* 7 (2006) 669–673.
- [10] N.L. Akers, C.M. Moore, S.D. Minter, *Electrochim. Acta* 50 (2005) 2521–2525.
- [11] A.S. Demir, F.N. Talpur, S.B. Sopaci, G.-W. Kohring, A. Celik, *J. Biotechnol.* 152 (2011) 176–183.
- [12] Y. Lu, Z.-I. Jiang, S.-W. Xu, H. Wu, *Catal. Today* 115 (2006) 263–268.
- [13] P.K. Addo, R.L. Arechederra, S.D. Minter, *Electroanalysis* 22 (2010) 807–812.
- [14] H. Wu, S. Huang, Z. Jiang, *Catal. Today* 98 (2004) 545–552.
- [15] Z. Jiang, S. Xu, H. Wu, *Stud. Surf. Sci. Catal.* 153 (2004) 475–480.
- [16] P.A. Munro, P. Dunnill, M.D. Lilly, *IEEE Trans. Magn.* 1 (1975) 1573–1575.
- [17] C.G.C.M. Netto, E.H. Nakamatsu, L.E.S. Netto, M.A. Novak, A. Zuin, M. Nakamura, K. Araki, H.E. Toma, *J. Inorg. Biochem.* 105 (2011) 738–744.
- [18] A. Manrich, A. Komesu, W.S. Adriano, P.W. Tardioli, R.L.C. Giordano, *Appl. Biochem. Biotechnol.* 161 (2010) 455–467.
- [19] J.T. Vivian, P.R. Callis, *Biophys. J.* 80 (2001) 2093–2109.
- [20] P.D. Adams, Y. Chen, K. Ma, M.G. Zagorski, F.D. Sönnichsen, M.L. McLaughlin, M.D. Barkley, *J. Am. Chem. Soc.* 124 (2002) 9278–9286.
- [21] S. D'Auria, J.R. Lakowicz, *Anal. Biotech.* 12 (2001) 99–104.
- [22] S. Chen, J.W. Burgner, J.M. Krahn, J.L. Smith, H. Zalkin, *Biochemistry* 38 (1999) 11659–11669.
- [23] N.E. Labrou, D.J. Rigden, *Biochem. J.* 354 (2001) 455–463.
- [24] V.O. Popov, V.S. Lamzin, *Biochem. J.* 301 (1994) 625–643.
- [25] J.S. Blanchard, W.W. Cleland, *Biochemistry* 19 (1980) 3543–3550.